JOURNAL OF MOLECULAR RECOGNITION
J. Mol. Recognit. 2004; **17**: 524–539
Published online 4 August 2004 in Wiley InterScience (www.interscience.wiley.com). DOI:10.1002/jmr.686

Review

Transient complexes of redox proteins: structural and dynamic details from NMR studies

Miguel Prudêncio and Marcellus Ubbink*

Leiden Institute of Chemistry, Leiden University, Gorlaeus Laboratories, PO Box 9502, 2300 RA Leiden, The Netherlands

Redox proteins participate in many metabolic routes, in particular those related to energy conversion. Protein–protein complexes of redox proteins are characterized by a weak affinity and a short lifetime. Two-dimensional NMR spectroscopy has been applied to many redox protein complexes, providing a wealth of information about the process of complex formation, the nature of the interface and the dynamic properties of the complex. These studies have shown that some complexes are non-specific and exist as a dynamic ensemble of orientations while in other complexes the proteins assume a single orientation. The binding interface in these complexes consists of a small hydrophobic patch for specificity, surrounded by polar, uncharged residues that may enhance dissociation, and, in most complexes, a ring or patch of charged residues that enhances the association by electrostatic interactions. The entry and exit port of the electrons is located within the hydrophobic interaction site, ensuring rapid electron transfer from one redox centre to the next. Copyright © 2004 John Wiley & Sons, Ltd.

Keywords: **cytochromes; electron transfer; redox enzyme; hydrophobic; electrostatic; iron-sulphur proteins; flavin proteins**

Received 20 January 2004; revised 6 April 2004; accepted 9 April 2004

INTRODUCTION

In the living cell protein–protein interactions help to fulfil a variety of biological processes. Interactions between proteins are not optimized to achieve the highest affinity, but rather to acquire the lifetime that is right for the molecular function of the protein complex. For example, for an inhibitor that binds to an enzyme, it can be important to shut down enzyme activity completely and thus a long-lived complex is necessary. This is achieved by a very high affinity between inhibitor and enzyme. In the case that two proteins have to react, a short lifetime is required to ensure a rapid turnover. Examples of such transient complex formation are found among redox proteins. Redox enzymes catalyse redox reactions and electron transfer (ET) proteins transfer electrons between them. The complexes formed between these proteins are characterized by dissociation rate constants of up to $10^4\,s^{-1}$, so the lifetimes are as short as 100 μs. Special features of the molecular interactions are necessary to guarantee the formation of a specific complex with reasonable affinity in such a short time. For example, many of these complexes employ electrostatic attraction to increase the association rate constant to the diffusion limit. By attraction and preorientation of the proteins upon their encounter, the number of productive collisions can be increased by several orders of magnitude, as was demonstrated by many kinetic studies on complexes of redox proteins.

The application of modern, two-dimensional NMR spectroscopy using ^{15}N-enriched proteins to study redox complexes has yielded new insights into the mechanisms of transient complex formation. The high resolution of this technique makes it possible to produce detailed maps of the binding sites, thus identifying the type of residues in the interface. It is becoming increasingly clear that electrostatic interactions alone are not sufficient for a specific complex and that hydrophobic interactions are required as well. At the same time, the latter have to be limited to avoid high affinities and thus increased lifetimes.

In this paper, an overview is presented of recent two-dimensional NMR spectroscopy studies on redox protein complexes. Many earlier studies used one-dimensional proton NMR spectroscopy, in particular the paramagnetically shifted resonances in haem proteins. However, these will not be discussed here because such experiments provide little

*Correspondence to: M. Ubbink, Leiden Institute of Chemistry, Leiden University, Gorlaeus Laboratories, PO Box 9502, 2300 RA Leiden, The Netherlands.
E-mail: m.ubbink@chem.leidenuniv.nl

Contract/grant sponsor: EC RTN 'Transient'; *contract/grant number:* HPRN-CT-1999-00095.
Contract/grant sponsor: EC Marie Curie Programme; *contract/grant number:* HPMF-CT-2000-00928.
Contract/grant sponsor: Netherlands Organisation for Scientific Research; *contract/grant number:* 700.52.425.

Abbreviations used: 2D, two-dimensional; AdR, adrenodoxin reductase; Adx, adrenodoxin; Cb_5, cytochrome b_5; Cc, cytochrome *c*; Cc_3, cytochrome c_3; Cc_{552}, cytochrome c_{552}; Cc_{553}, cytochrome c_{553}; Cc_6, cytochrome c_6; CcP, cytochrome *c* peroxidase; Cf, cytochrome *f*; CHmc, cytochrome Hmc; CP450cam, cytochrome P450cam; CP450scc, cytochrome P450scc; *Dn*, *Desulfomicrobium norvegicum*; *Dv*D, *Desulfovibrio desulfuricans* ATCC 7757; *Dv*H, *Desulfovibrio vulgaris* Hildenborough; ET, electron transfer; FAD, flavin adenine dinucleotide; Fd, ferredoxin; FDH, formate dehydrogenase; FdxI, ferredoxin I; FeHase, [Fe]-hydrogenase; FNR, ferredoxin-$NADP^+$ oxidoreductase; Mb, myoglobin; Pc, plastocyanin; PdR, NADH-putidaredoxin reductase; Pdx, putidaredoxin.

information about the nature of the interface. A brief introduction into the use of two-dimensional NMR spectroscopy for the study of protein complexes is provided below. More advanced methods are described briefly, where appropriate, but it is outside the scope of this review to discuss these methods in detail and the reader is referred to the original papers. After the section introducing the NMR methods, a general model is presented that may help to understand the results for the various complexes described afterwards. Finally, the new insights into the process of transient complex formation will be summarized.

NMR SPECTROSCOPY AND TRANSIENT PROTEIN COMPLEXES

NMR spectroscopy is particularly suited for the study of low affinity complexes. In a chemical-shift perturbation experiment, a ^{15}N-labelled protein is selectively monitored during a titration with the unlabelled partner. Complex formation gives rise to changes in the chemical environment of nuclei at the interface, such that the chemical shift (δ) of these nuclei differs between the bound (δ_{bound}) and free (δ_{free}) forms. The effects on the NMR spectrum are dependent on the lifetime of the complex. In the slow exchange limit, the lifetime of the complex is long relative to the difference (in rad s^{-1}) between δ_{bound} and δ_{free} ($\Delta\delta_{Max}$) and the nucleus in the bound and the free state of the protein resonates at δ_{bound} and δ_{free}, respectively [Fig. 1(A, B)]. Upon titration of the partner protein, the resonance intensity decreases at δ_{free} and increases at δ_{bound}, proportionally to the fraction of bound protein. If the exchange is moderately slow, both resonances may experience line broadening. In the fast exchange limit, the lifetime is much shorter than $\Delta\delta_{Max}$ and a single resonance is observed at the weighted average of δ_{bound} and δ_{free} [Fig. 1(C, D)]. During a titration, the ratio of the two proteins is altered and thus the fraction of bound protein changes. In the case of fast exchange, this results in a proportional shift of the average peak; as the fraction of bound protein increases, δ approaches δ_{bound} and thus the change in δ ($\Delta\delta_{Bind}$) approaches $\Delta\delta_{Max}$.

The lifetime is determined by the dissociation rate constant k_{off}. Generally, in transient complexes of electron transfer proteins, the fast exchange regime is observed, so $k_{off} > \Delta\delta_{Max}$ for most peaks (note that $\Delta\delta_{Max}$ is different for each nucleus) and a lower limit for k_{off} can be set at $\sim 200\,s^{-1}$.

When $\Delta\delta_{Bind}$ is plotted as a function of the molar ratio of the reactants, it is possible to derive binding curves for complex formation and hence the stoichiometry and affinity

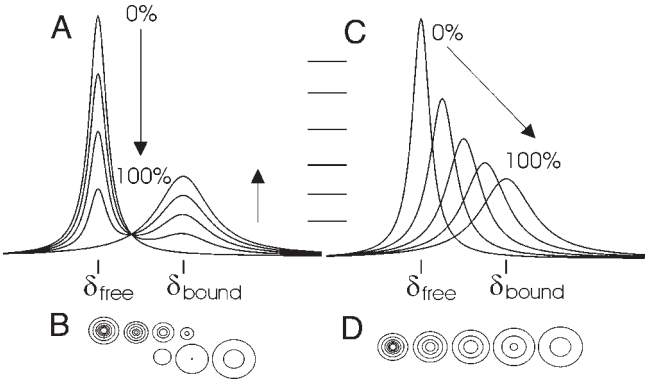

Figure 1. Slow and fast exchange. In the slow exchange limit (A, B) a nucleus that experiences different resonance frequencies in the free state (δ_{free}) and in the bound state (δ_{bound}) exhibits two resonances with intensities that are proportional to the fraction of free and bound states. The linewidths are determined by the rotational correlation time (and thus by the size and shape) of the free protein and the complex. In the fast exchange limit (C, D), the nucleus exhibits a single resonance at an averaged position weighted by the fractions of bound and free protein. The linewidth is also the weighted average of the linewidth in the free and bound states. The curves represent the 0, 25, 50, 75 and 100% bound state. For the bound state a linewidth three times that of the free state was used. (B, D) The contour plots of the peaks shown in (A) and (C), with the contour levels indicated by the horizontal lines in the centre of the figure. The contours give an impression of the appearance of the resonances in a 2D-NMR spectrum.

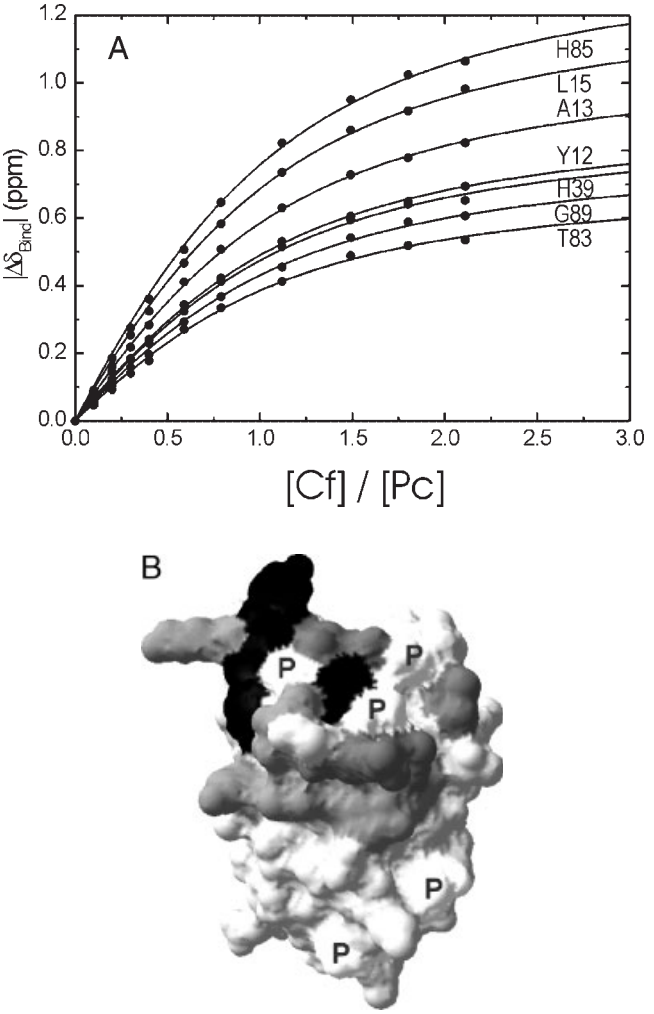

Figure 2. Binding curves and interface map. (A) Chemical-shift perturbation curves for residues of *Prochlorothrix hollandica* Pc in a titration with *Phormidium laminosum* Cf. The curves were fitted to a single binding constant of $6(\pm 2) \times 10^3\,M^{-1}$ (Crowley *et al.*, 2002c). (B) Binding map of the binding site for Cf on Pc, with the size of the chemical-shift perturbations of the amide groups grey-coded onto the surface representation of Pc (Babu *et al.*, 1999; PDB entry 2b3i), with the darkest areas indicating the residues with the largest perturbations. P, prolines (no data available).

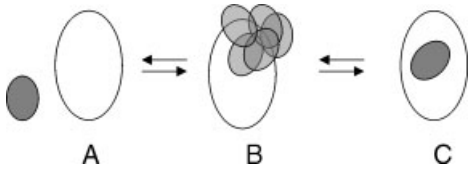

Figure 3. Model for complex formation. (A) Free proteins. (B) Encounter complex consisting of a dynamic ensemble of orientations. In this state, very small chemical-shift perturbations are observed. (C) Reactive complex, in which the proteins assume a well-defined orientation in the complex. Large perturbations are observed for this state. Reprinted from Ubbink *et al.* (1998), Copyright (1998), with permission from Elsevier.

can be determined. In Fig. 2(A), $|\Delta\delta_{\mathrm{Bind}}|$ is plotted for several amide nuclei of plastocyanin (Pc) when titrated with cytochrome *f* (Cf). With increasing ratio of Cf over Pc, the fraction of bound Pc increases and $\Delta\delta_{\mathrm{Bind}}$ approaches $\Delta\delta_{\mathrm{Max}}$. The percentage of bound protein can be calculated from the ratio of the experimentally observed $\Delta\delta_{\mathrm{Bind}}$ and the fitted $\Delta\delta_{\mathrm{Max}}$. In order to compare chemical-shift perturbations in different complexes, often the shifts are extrapolated to the 100% bound form ($\Delta\delta_{\mathrm{Max}}$) and the average chemical-shift perturbation ($\Delta\delta_{\mathrm{Avg}}$) is calculated for each backbone amide using:

$$\Delta\delta_{\mathrm{Avg}} = \sqrt{[(\Delta\delta\mathrm{N}/5)^2 + \Delta\delta\mathrm{H}^2]/2} \qquad (1)$$

where $\Delta\delta$N and $\Delta\delta$H are the changes in the ^{15}N and $^{1}\mathrm{H}^{\mathrm{N}}$ chemical-shifts, respectively, when the protein is 100% bound. A picture of the interaction interface can be obtained by mapping $\Delta\delta_{\mathrm{Avg}}$ to a surface representation of the protein, as illustrated in Fig. 2(B).

In addition to chemical-shift perturbation, complex formation in the fast exchange regime is manifested as a general broadening of the resonances. The rotational correlation time of the complex is larger than that of the free proteins, resulting in an increase in the line widths of all resonances. As with chemical shifts, in the fast exchange limit, the line width of the average resonance is the weighted average of the line widths of the free and bound forms [Fig. 1(C, D)].

A MODEL FOR COMPLEX FORMATION

In the generally accepted view, two proteins first form an encounter complex, before the reactive complex is formed (Fig. 3). The encounter complex [Fig. 3(B)] is best described as an ensemble of orientations, in particular in complexes with strong electrostatic attraction. In these proteins, the charges generally form a patch or ring on both proteins. Upon approach, the electrostatic force orients the proteins such that the oppositely charged patches are facing each other. However, the electrostatic forces are long-range, resulting in many orientations that have approximately equal energy and thus represent an ensemble of orientations. Within the encounter complex the proteins are diffusing over part of the surface of the partner protein. The interactions in the encounter complex are weak and averaged over all the orientations. It can be expected that these have very little effect on the NMR spectrum. The dominant effects of complex formation observed in the NMR spectrum result from the reactive complex [Fig. 3(C)]. This is a well-defined complex, in which hydrophobic interactions are important. The stronger molecular interactions and, in particular, changes in the solvation state of the interface residues may be the reasons for the chemical-shift perturbations.

We have found surprising differences in the average size of the perturbations between complexes. Figure 4 illustrates this for the complexes of cytochrome *c* peroxidase and cytochrome *c* and of cytochrome b_5 and myoglobin (Worrall *et al.*, 2002). Using the model discussed above, this

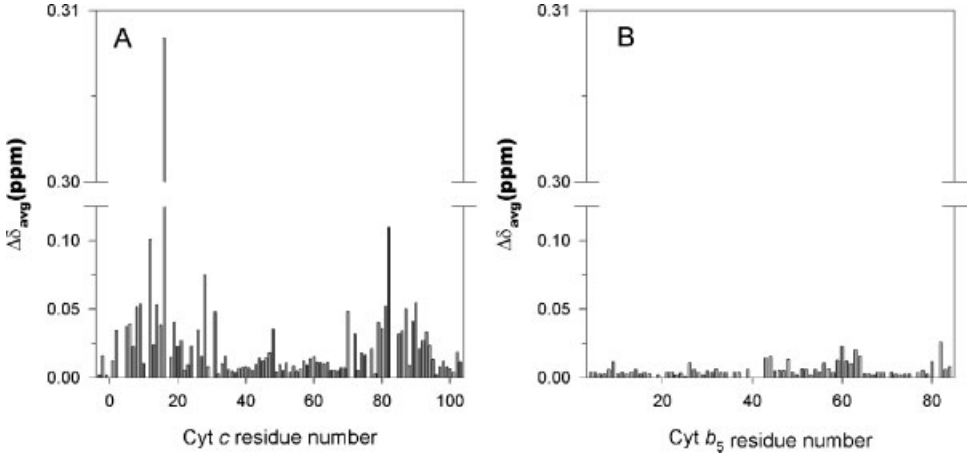

Figure 4. Chemical-shift perturbations in two complexes. The amide chemical-shift perturbations ($\Delta\delta_{\mathrm{avg}}$) extrapolated to 100% bound form are shown for all observed residues of Cc (Cyt *c*) in complex with CcP (A) and for Cb_5 (Cyt b_5) in complex with Mb (B). Note the large difference in the average perturbation between the complexes, suggesting that the CcP–Cc complex is mostly in a single orientation (state C in Fig. 3) and the Mb–Cb_5 complex is a dynamic ensemble of orientations. Reprinted with permission from Worrall *et al.* (2002). Copyright (2002) American Chemical Society.

can be interpreted as evidence that some complexes exist predominantly as an ensemble of orientations, so they only form an encounter complex [very small perturbations, Fig. 4(B)], while others exist partly, predominantly or almost entirely as single-orientation complex [large perturbations, Fig. 4(A)]. In other words, the equilibrium between states B and C in Fig. 3 can be either towards B or C. The complexes that are entirely in the B state could be called non-specific; those that populate also the C state are specific.

CYTOCHROME *c* PEROXIDASE AND CYTOCHROME *c*

Yeast mitochondrial cytochrome *c* peroxidase (CcP) catalyses the reduction of peroxides, with electrons that are donated by cytochrome *c* (Cc). CcP (34 kDa) contains a single, non-covalent haem, which is buried deep under the protein surface. Cc is a small (12.5 kDa) electron transfer protein with a single haem group that is covalently attached to the protein via two thioether bridges. The complex is a paradigm for electron transfer protein complexes and it has been the subject of many kinetic, spectroscopic and structural studies. CcP appears to have two binding sites for Cc, one much stronger (K_d in the low μM range), but less efficient in ET than the other (K_d in the mM range; Zhou and Hoffman, 1994; Zhou *et al.*, 1995; Nocek *et al.*, 1996). The CcP–Cc complex is one of the few electron transfer complexes for which a crystal structure is available (Pelletier and Kraut, 1992; PDB entry 2pcc), which is believed to represent the tight binding site. The interface is centred around residue Ala194 of CcP and residue Gly83 of Cc. It comprises both polar and hydrophobic residues, as well as two charge–charge interactions. The approximate location of the second binding site has been determined by site-directed mutagenesis, and involves residues 146–150 (Leesch *et al.*, 2000).

Early NMR spectroscopy studies have demonstrated that the dissociation rate of the complex is concentration dependent (Moench *et al.*, 1992; Yi *et al.*, 1994a), indicating that complex formation is not a simple bimolecular process. The first two-dimensional mapping of the binding site on Cc was performed by taking advantage of the protection against solvent exchange of amide protons in the interface upon complex formation. When Cc is brought into deuterated water, each amide proton will be exchanged to a deuteron with a rate that depends on the environment of the proton. Buried and hydrogen-bonded amide protons exchange much slower than exposed ones. Upon complex formation amide protons in the interface demonstrate decreased exchange rates, because they become protected from the solvent. The protection factors (the ratio of the exchange rates for bound and free Cc) were as high as 40 for yeast Cc in complex with CcP (Yi *et al.*, 1994b), but only 10 or lower for the complex of horse Cc with yeast CcP (Jeng *et al.*, 1994), suggesting that the latter, non-physiological complex is more dynamic. These studies indicated that the front face of Cc, i.e. near the haem edge, involving residues in the so-called 10s and 70s helices, are part of the interface (Yi *et al.*, 1994b). However, some residues on the opposite side of Cc also showed increased protection.

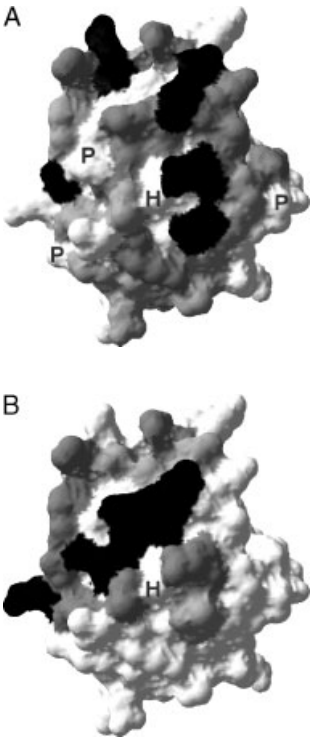

Figure 5. The binding site of cytochrome *c* for cytochrome *c* peroxidase. (A) Chemical-shift perturbation map of the effects on ferric Cc upon complex formation with CcP based on the data from Worrall *et al.* (2001). Cc (Berghuis and Brayer, 1992; PDB entry 2ycc) is shown in a surface representation with the residues grey-coded according to the size of the perturbations, with the darkest areas indicating the residues with the largest perturbations. P, prolines (no data available), H, haem edge. (B) Interface of Cc in the crystal structure of the Cc-CcP complex. Residues in black, dark grey and light grey are within 4, 5 and 6 Å of CcP atoms, respectively. The haem egde is marked with a H. The figure was produced with Swiss PDB-Viewer.

The interface of the complex in solution has also been mapped using two-dimensional chemical-shift perturbation of Cc amide resonances (Worrall *et al.*, 2001). The binding maps of the reduced and oxidized Cc with CcP(FeIII) are similar, although not identical. Both involve the front face of Cc and, in particular, the uncharged polar and hydrophobic residues around the haem edge. The perturbations are somewhat larger for the oxidized Cc and spread more to the sides of the protein. This suggests that there are subtle differences in the structure or dynamics of the complex depending on the redox state of Cc. A comparison of the interface found in the crystal structure and in solution is shown in Fig. 5. The interfaces are similar, although more extended in the one determined by NMR spectroscopy. Yet, it can be concluded that, at least from the point of view of Cc, the crystal structure is a reasonable representation of the structure in solution. In the crystal structure of the complex it was found that the side chain of Cc residue Gln16 had folded back to form a hydrogen bond with its backbone amide. By far the biggest shift in the NMR spectrum was observed for this particular backbone amide, suggesting that this hydrogen bond is also formed in solution. In this study it was also shown that the size and orientation of the magnetic susceptibility tensor of oxidized Cc are not changed upon complex formation, indicating the absence of any significant changes in the haem electronic structure.

COMPLEXES OF CYTOCHROME *f* WITH PLASTOCYANIN AND CYTOCHROME c_6

In the photosynthetic redox chain, electrons are transferred from the b_6f complex to either Pc or cytochrome c_6 (Cc_6). The latter two are both small soluble proteins that transfer electrons from the b_6f complex to photosystem I. Although functionally the same, structurally these proteins are very different. Pc is largely a β-sheet protein, containing a single copper as redox centre, while Cc_6 is a small α-helical *c*-type cytochrome, similar to mitochondrial Cc. In algae and cyanobacteria that produce both Pc and Cc_6 functional convergence is observed; both proteins from the same organism share the same pI and surface properties (Hervás *et al.*, 2003). Crystal and NMR structures have been determined for many plastocyanins (Freeman and Guss, 2001) and several cytochromes c_6 (Reuter and Wiegand, 2001) as well as for the soluble domain of several cytochromes *f* (Soriano *et al.*, 2001). Recently, the structure of the complete cytochrome b_6f complex was reported (Kurisu *et al.*, 2003; PDB entry 1 um3). Many kinetic studies have been performed to characterize the interaction of both the complete b_6f complex and the isolated soluble domain of Cf with their redox partners (see Hope, 2000; Illerhaus *et al.*, 2000; Hart *et al.*, 2003 and references therein). It has been demonstrated that, in the case of plants and green algae, the interaction of Cf with Pc is strongly dependent on ionic strength although *in vivo* studies on the green alga *Chlamydomonas reinhardtii* did not support this finding (Soriano *et al.*, 1996). In cyanobacteria the interactions between Cf and both Pc and Cc_6 are more diverse. In *Phormidium laminosum* the complex of Cf and Pc is nearly independent of ionic strength effects (Crowley *et al.*, 2001; Schlarb-Ridley *et al.*, 2002), but for example in *Anabaena* the affinity in the complexes of Cf with both Pc and Cc_6 is dependent on ionic strength (M. Ubbink and I. Diaz-Moreno, unpublished results).

Chemical-shift perturbation studies (Ubbink *et al.*, 1998; Ejdebäck *et al.*, 2000; Crowley *et al.*, 2001; Bergkvist *et al.*, 2001) demonstrate that invariably the hydrophobic patch of Pc is involved in complex formation. This is a small area surrounding an exposed His residue, which is a ligand of the copper ion, suggesting that a small hydrophobic patch is used to form a specific complex with the partner, bringing the entry/exit port for electrons, the His residue, in close contact with the partner. A similar pattern is observed in the complex of CcP and Cc, with the hydrophobic and uncharged polar residues around the haem edge (see Fig. 5). In the case of plants, distinct effects are seen also for the acidic patch region of the surface, suggesting that also this side of the protein is part of the interface.

When cadmium-containing Pc is used as a redox inactive substitute of copper Pc, the chemical-shift perturbations caused by both oxidized and reduced Cf can be determined without interference of ET reactions during the NMR experiment. When oxidized Cf was added, additional shifts were observed that were all localized in the hydrophobic patch. It was shown that these additional shifts are a consequence of the paramagnetic state of the haem. These shifts are so-called intermolecular pseudocontact shifts (Bertini and Luchinat, 1996), resulting from the dipolar interaction of the unpaired electron on the haem and the magnetic spin of the Pc protons. The pseudocontact shifts depend on the distance between the haem iron and the protons in Pc and could thus be used to determine the orientation of Pc relative to Cf in the complex (Ubbink *et al.*, 1998; Crowley *et al.*, 2001). The hydrophobic patch of Pc is localized close to the haem of Cf, with an iron-copper distance of 11 and 15 Å in the complexes from plant and *P. laminosum*, respectively (Fig. 6). This interface consists mainly of hydrophobic and uncharged polar residues. In the plant case, the acidic patch on the side of the Pc also makes contact with Cf, establishing electrostatic interactions. In the *P. laminosum* case, the Pc demonstrates a head-on orientation, with the interface limited to the hydrophobic patch (see Fig. 6), in agreement with the reduced importance of electrostatic interactions in this complex.

The importance of the shape of the hydrophobic patch was evaluated in a mutagenesis study (Crowley *et al.*, 2002c). *Prochlorothrix hollandica* Pc is an exceptional plastocyanin in that it has a Tyr and a Pro residue at positions 12 and 14 where most other plastocyanins have a Gly and a Leu residue, respectively. The interaction of the

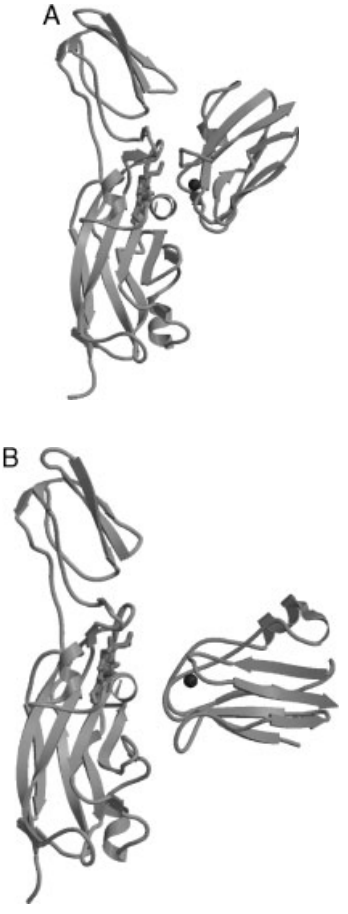

Figure 6. The complex plastocyanin and cytochrome *f*. Ribbon representation of the complexes of Pc (right) and Cf (left) from plant (A, PDB entry 1pcf; Ubbink *et al.*, 1998) and the cyanobacterium *P. laminosum* (B) (Crowley *et al.*, 2001). The haem in Cf is shown as a stick model and the copper is Pc is represented by a sphere. Note the difference in the orientation of Pc in the two complexes.

wild-type Pc and the Y12G/P14L double mutant with *P. laminosum* Cf was studied with NMR spectroscopy. The affinity of wild-type and mutant Pc for Cf were the same ($K_d = 160\,\mu M$) and the binding maps were similar. The average chemical-shift perturbation was, however, reduced in the mutant, which could indicate an increased dynamics due to the smoother hydrophobic patch in the mutant. It should be noted that a non-physiological Cf was used, so the effects could be different in the physiological complex.

The heterologous complexes of *P. laminosum* Cf and cytochromes c_6 from *Synechococcus elongatus* and *Anabaena* sp. PCC 7119 have also been studied by NMR spectroscopy (Crowley *et al.*, 2002a). The cytochromes *f* of these three cyanobacteria have very similar amino acid sequences and predicted pI values, but the cytochromes c_6 differ in overall charge, with pIs of 4.8 and 9.0 for *S. elongatus* and *Anabaena* Cc_6, respectively. As a result, the former shows no complex formation with Cf, while the latter associates with a K_d of about $120\,\mu M$. The binding interface of Cc_6 consists of uncharged polar and hydrophobic residues located around the exposed haem edge, very similar to what was observed for Cc in the complex with CcP. Residues Cys17, Met58 and Ala60 exhibit the largest shifts. Molecular docking calculations based on these results suggested that Cc_6 binds close to the haem group of Cf (Crowley *et al.*, 2002a). A similar study on the non-physiological complex of yeast Cc and *P. laminosum* Cf had demonstrated that Cc can bind at the same position, as well as at the 'backside' of Cf. Yeast Cc binds Cf with the region around the haem edge, like in the complex with CcP (Crowley *et al.*, 2002b).

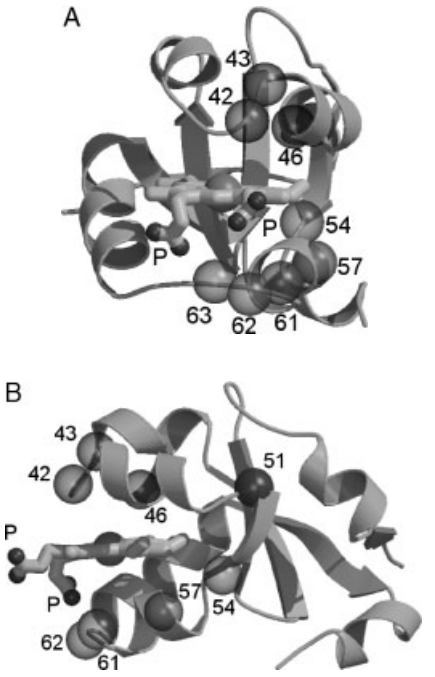

Figure 7. Cytochrome b_5. Front (A) and side view (B) of the soluble domain of bovine Cb_5 (Durley and Mathews, 1996; PDB entry 1cyo), with the haem in sticks. P, propionate oxygens. The semi-transparent spheres represent amide nuclei with the residue numbers mentioned in the text, with 54, 57, 61–63 indicating the amides of which the dynamic properties change upon complex formation (Shao *et al.*, 2003). The figure was produced with MOLSCRIPT (Kraulis, 1991) and Raster3D (Merrit and Bacon, 1997).

COMPLEXES OF CYTOCHROME b_5 WITH CYTOCHROME *c* AND MYOGLOBIN

Cytochrome b_5 (Cb_5) is a low-spin haem protein responsible for ET reactions in a number of physiological processes. It exists both in membrane-bound and in soluble form. The membrane-bound form is located in the endoplasmic reticulum and the mitochondrial membrane, and consists of a hydrophilic domain (9 kDa) that harbours a *b*-type haem, and a short membrane anchor. In the endoplasmic reticulum it provides reducing equivalents for fatty acid desaturation, cholesterol biosynthesis and the oxidation of certain substrates by cytochromes P-450. Trypsin proteolysis of membrane-bound Cb_5 produces the soluble N-terminal fragment, consisting of 84 residues, of which several X-ray crystal structures have been determined (Fig. 7).

The interaction of the soluble domain of Cb_5 with Cc has been studied extensively, serving as a model for ET complexes in general. It is outside the scope of this review to discuss all the earlier work (see Banci *et al.*, 2003; Shao *et al.*, 2003 for an overview). We will focus on the recent two-dimensional NMR spectroscopy studies that have enabled a detailed mapping of the binding sites on both Cb_5 and Cc. The first study using ^{15}N-labelled Cb_5 demonstrated that intermolecular pseudocontact shifts can be observed on Cb_5 when the perturbations caused by the paramagnetic, oxidized form of Cc are compared with those caused by diamagnetic, reduced Cc (Guiles *et al.*, 1996). Unfortunately, the dynamics within the complex limit the application of these shifts for structure calculation. Analysis of the complex of bovine Cb_5 and horse Cc (Hom *et al.*, 2000; Shao *et al.*, 2003) indicated small but extensive chemical shift perturbation of Cb_5 residues, covering both the area around the exposed haem propionate groups and the region on the 'side' of the protein, centred around residue 51 (Fig. 7; Hom *et al.*, 2000). These perturbation studies have been complemented with relaxation experiments on the complex with both proteins in the reduced form, indicating a decreased mobility on the μs to ms timescale of the α-helix comprising residues 54–63 upon complex formation (Shao *et al.*, 2003). A cross-saturation experiment (Takahashi *et al.*, 2000), in which magnetisation saturation is transferred from Cc to Cb_5 amide nuclei in the interface, highlighted the involvement of several other residues, Gly42, Glu43 and Leu 46 (Shao *et al.*, 2003; Fig. 7). On the basis of these results it was concluded that a 1:1 complex is formed, with the main site of interaction around the exposed haem propionates, similar to the models proposed by Salemme (1976) and Mauk and co-workers (Northrup *et al.*, 1993).

Somewhat different results were obtained for the complex of reduced rabbit Cb_5 with reduced yeast Cc (Banci *et al.*, 2003). The chemical-shift perturbations are of similar size and also rather extensive, but cover a somewhat different surface area. Measurements of the rotational correlation time under various conditions provide strong evidence for a complex in which two Cc molecules can bind to one Cb_5, with the second binding site being much weaker

than the first. In this study, the perturbations on Cc were also measured, showing that Cc binds using the haem edge, similar though not identical to the interface found for the complex of Cc with CcP (*vide supra*). Molecular modelling of the binding site on Cb_5 on the basis of the experimental results suggested a major interaction site on the side of this protein, i.e. away from the haem propionates.

In summary, it is clear that various studies yield somewhat different results, and a unique, relatively well-defined binding site like observed in complexes of Ccp–Cc, Cf–Pc and Cf–Cc_6, is probably absent in the case of Cb_5–Cc. The precise effects vary between cytochromes from different species. The sizes of the chemical-shift perturbations and the extent of surface area affected also suggest that the complex is dynamic, and thus predominantly in the B-state shown in Fig. 3.

It has been suggested that Cb_5 also functions in a repair process, to reduce haemoglobin and myoglobin that have been oxidized accidentally to the Fe(III) state (Hagler *et al.*, 1979; Livingston *et al.*, 1985). Kinetic studies of the complex with native Mb and with Mb in which the haem propionates had been neutralized, in parallel with Brownian dynamics and ET pathways calculations, led to the development of a new 'dynamic docking' model for highly dynamic protein–protein complexes (Liang *et al.*, 2002). This model postulates that Cb_5 binds to a large area on the Mb surface, in a wide variety of conformations, like in the B-state in Fig. 3. There is no specific or favoured orientation for this complex, but only a small subset of its many conformations are ET-active, and these have Cb_5 bound in the vicinity of the haem edge. This model found support in a recent NMR spectroscopy study on bovine Cb_5 and Mb (Worrall *et al.*, 2002), which showed that complex formation can be detected, both by chemical-shift perturbations and by correlation time measurements. The perturbations were very small [Fig. 4(B)] and spread over a large part of the surface of Cb_5, suggesting a highly dynamic complex. Molecular modelling on the basis of these NMR spectroscopy results indicated that Cb_5 has some preference to bind around the exposed parts of the haem of Mb, but does not assume a well-defined orientation in the complex.

CYTOCHROME c_{552} AND THE Cu_A DOMAIN OF CYTOCHROME *c* OXIDASE

In the respiratory chain, electrons flow from the cytochrome bc_1 complex (complex III) to haem type aa_3 cytochrome *c* oxidase (complex IV), in which they are used to reduce dioxygen to water. In mitochondria, the electron transport is catalysed by Cc, while in the Gram-negative bacterium *Paracoccus denitrificans*, the membrane-anchored cytochrome c_{552} (Cc_{552}) performs this role. The interaction between the soluble domain of Cc_{552} and the copper-containing soluble domain of the second subunit of cytochrome *c* oxidase was analysed using chemical-shift perturbation (Wienk *et al.*, 2003) of the Cc_{552} amide resonances. The predominant effects are observed for non-polar residues situated around the exposed haem edge. The chemical-shift changes, which were observed in a sample with 0.5 mM Cc_{552} and 2.2 mM of the Cu_A domain, were very small. This could imply either that the complex is a dynamic ensemble of orientations (see above), like the complex of Mb and Cb_5, or that the affinity is very weak (no binding constant was reported). The surface map of the shifts is quite extensive, which is evidence for a dynamic ensemble. However, a low affinity is also a real possibility, since both proteins are normally membrane-bound and thus exhibit only two-dimensional diffusion and have a high local concentration. This may limit the need for a high affinity. We have observed this in a similar case, with two membrane bound proteins, the azurin and the nitrite reductase from *Neisseria*, which in solution showed no significant complex formation (M. Ubbink and A. Impagliazzo, unpublished results). It cannot be excluded that Cc_{552} interacts not only with the Cu_A domain, but also with subunit I of the cytochrome *c* oxidase. This could enhance both the affinity and the specificity of the interaction.

CYTOCHROME c_{553} COMPLEXES WITH FERREDOXIN I AND [Fe]-HYDROGENASE

The monohaem cytochrome c_{553} (Cc_{553}) is a 9.5 kDa, low potential, *c* type cytochrome that acts as redox partner of formate dehydrogenase (FDH; Sebban *et al.*, 1995) and [Fe]-hydrogenase (FeHase; Verhagen *et al.*, 1994) in the sulphate-reducing bacterium *Desulfovibrio vulgaris* Hildenborough (*Dv*H). The lysine distribution on the surface of Cc_{553}, in conjunction with studies of ionic strength dependence for complex formation, suggests that electrostatic interactions play an important role in the formation of the complexes between the cytochrome and FDH (Sebban-Kreuzer *et al.*, 1998b) or FeHase (Morelli *et al.*, 2000a). The solution structure of *Dv*H Cc_{553} is available (Marion *et al.*, 1995; Blackledge *et al.*, 1995; PDB entry 1dvh) and was used in the docking studies reported hereafter.

Both FDH and FeHase contain a ferredoxin-like domain that presents 27 and 30% identity, respectively, with ferredoxin I (FdxI) from *Desulfomicrobium norvegicum* (*Dn*; formerly *Desulfovibrio desulfuricans*, Norway strain). *Dn* FdxI, a 6.2 kDa protein containing a [4Fe–4S] cluster, is an obligate intermediate in *Dv*H Cc_{553} reduction by pyruvate dehydrogenase (Blanchard *et al.*, 1993). For this reason, *Dn* FdxI has been chosen as a model for the 'ferredoxin-like' domain of FDH and Fe-Hase, to study the general features of the recognition between Cc_{553} and its redox partners. The structural model for *Dn* FdxI used in the docking calculations described below was constructed on the basis of the homology with ferredoxin II from *Desulfovibrio gigas*, of which crystal (Kissinger *et al.*, 1991) and solution (Goodfellow *et al.*, 1999) structures are available (PDB entries 1fxd and 1f2g, respectively).

The effects of the addition of *Dv*H Cc_{553} to *Dn* FdxI on the latter were followed by 1D NMR spectroscopy and revealed a 1:1 stoichiometry and a dissociation constant of 3 μM for this complex (Morelli and Guerlesquin, 1999). 2D NMR spectroscopy allowed the interaction sites on Cc_{553} (Morelli and Guerlesquin, 1999) and on FdxI (Morelli *et al.*, 2000b) to be mapped (Fig. 8). Using a combined *ab initio*/

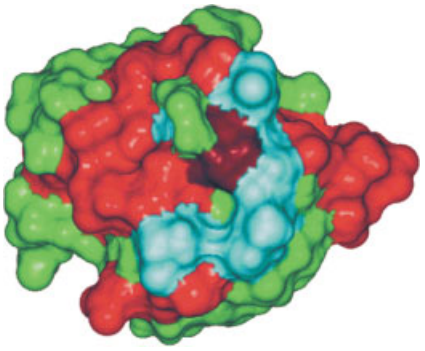

Figure 8. Binding site for cytochrome c_{553} on ferredoxin I. Map of the interaction site for Cc_{553} on FdxI (based on PDB entry 1fxd). Residues that undergo chemical-shift perturbations are coloured in red; the Cys12, which is perturbed in 1D-NMR experiments, is shown in brown. In green are the unaffected residues and in blue the unassigned amide groups. Reprinted with permission from Morelli *et al.* (2000b). Copyright (2000) American Chemical Society.

Figure 9. Model of the complex formed between FdxI and FeHase. FeHase is coloured in black, with the ferredoxin-like domain in light grey. The 2Fe and Fe–S clusters on FeHase are represented as spheres and the haem group on Cc_{553} is represented as a stick model. The picture was generated on the basis of PDB entry 1hfe (Morelli *et al.,* 2000a) with the program YASARA and rendered with PovRay.

experimental approach, the docking program BiGGER (Palma *et al.*, 2000; Morelli *et al.*, 2001; Krippahl *et al.*, 2003) was employed to dock the Cc_{553} and FdxI. It was suggested that a dynamic ensemble of orientations may occur upon binding, based on the fact that no single structure was found to fulfil all 19 available NMR constraints simultaneously (Morelli *et al.*, 2000b). A model was proposed (PDB entry 1dwl) in which the interface involves a surface patch surrounding the heme crevice on Cc_{553} and the two parallel alpha helices accommodating the Fe–S cluster on the FdxI, with the two redox centres facing each other, at a distance of 10.0 Å. This model is in agreement with site-directed mutagenesis studies that showed that the Lys62 and Lys63 residues of Cc_{553} are involved in the interaction with FDH (Sebban-Kreuzer *et al.*, 1998b) and that Tyr64 is required for electron transfer to this enzyme (Sebban-Kreuzer *et al.*, 1998a).

The FdxI–Cc_{553} complex was shown to be a good model for the interacting domain of Cc_{553} with FeHase. 2D NMR experiments data were combined with BiGGER docking calculations to study the interaction of *Dv*H Cc_{553} with the 54 kDa FeHase from *Desulfovibrio desulfuricans* ATCC 7757 (*Dv*D), which is assumed to be identical to the homologous enzyme from *Dv*H (Morelli *et al.*, 2000a). The crystal structure of *Dv*D FeHase (Nicolet *et al.*, 1999; PDB entry 1hfe) shows that the enzyme comprises two different subunits of 42.5 and 11 kDa, with the large subunit harbouring a ferredoxin-like domain composed of two [4Fe–4S] clusters and an active Fe–S centre, termed the H cluster. Transverse relaxation-optimized spectroscopy (TROSY) (Pervushin *et al.*, 1997; Fernandez and Wider, 2003) NMR experiments were performed to map the interacting site of the cytochrome. These NMR data were used in conjunction with the program BiGGER to generate a model of the interaction between the two proteins (Fig. 9). According to this model (PDB entry 1e08), the interaction of Cc_{553} with the ferrodoxin-like domain of FeHase is very similar to the one found for the Cc_{553}–FdxI complex, with the heme and the distal Fe–S centre (the one conserved in the mononuclear ferredoxins) 12 Å apart. The interacting surface includes the environment of the axial methionine (Met57) of the cytochrome (Morelli *et al.*, 2000a).

HYDROGENASE–CYTOCHROME c_3–CYTOCHROME Hmc

Cytochrome c_3 (Cc_3, 13 kDa) is a periplasmic low potential cytochrome that occurs in sulphate-reducing bacteria. The structure of Cc_3 from *Dv*H has been determined and is available under PDB accession number 2cth (unpublished results). Cc_3 contains four haem groups and has been suggested to act as an electron shuttle between FeHase and cytochrome Hmc (CHmc; Aubert *et al.*, 2000). CHmc is a periplasmic, high-molecular-weight cytochrome containing 16 haem groups. The X-ray structure of *Dv*H CHmc (Czjzek *et al.*, 2002; PDB entry 1gws) revealed a modular organization in three domains: the N-terminal domain I, homologous to the 3-haem-containing cytochrome c_7; domain II, similar to cytochromes of the c_3 type; and the C-terminal domain III, with a spatial arrangement similar to that of the 9-haem-containing cytochrome Hcc.

Complex formation of CHmc and Cc_3 was monitored by measuring the chemical-shift perturbations on the [^{1}H-^{15}N]-HSQC spectrum of ^{15}N-labelled Cc_3 (Czjzek *et al.*, 2002). Ten residues on Cc_3 were found to be affected by CHmc. These NMR results were used as constraints to filter the solutions obtained from *ab initio* BiGGER docking simulations and thereby generate a structural model of the interaction between the two proteins (Czjzek *et al.*, 2002). According to this model, Cc_3 interacts with domain III of CHmc and electron transfer takes place between haem 4 of the former and haem 616 of the latter. Similarly to what was found in the case of the FeHase–Cc_{553} complex (see previous section), the present model suggests that hydrophobic residues are found at the interface of Cc_3–CHmc interaction. Charged residues on both proteins (mostly lysines from Cc_3 and acidic residues from CHmc) are also found in the interface region, but in most cases, the model does not

predict that they are involved in direct charge–charge interactions.

The interaction between Cc_3 and FeHase has been studied following a 2D-NMR spectroscopy approach similar to that described for the Cc_3–CHmc interaction. Chemical-shift changes on the HSQC spectrum of ^{15}N-labelled Cc_3 upon addition of the FeHase were used to filter *ab initio* BiGGER docking simulations and generate a structural model for the Cc_3-FeHase complex (ElAntak *et al.*, 2003). The observed perturbations are consistent with a fast exchange process on the NMR time scale. Eleven Cc_3 residues were found to be significantly affected by the presence of FeHase. Five of these residues are also affected in the Cc_3–CHmc binding experiments (see above), suggesting that the same area of Cc_3 might be involved in both interacting sites. Again, hydrophobic residues appear to play an important role in the interaction and, in addition, several lysines in the loops surrounding haem 4 are involved in the interaction, in agreement with the idea that electrostatics are the driving force for the formation of complexes involving Cc_3 (Cambillau *et al.*, 1988; Stewart *et al.*, 1989). According to the model proposed for Cc_3–FeHase interaction, haem 4 of Cc_3 is the entrance gate of electrons to the cytochrome. These results, in conjunction with those obtained for the Cc_3–CHmc complex (Czjzek *et al.*, 2002), seem to exclude the possibility of ternary complex formation and, instead, favour the idea of Cc_3 acting as an electron shuttle between FeHase and CHmc (ElAntak *et al.*, 2003).

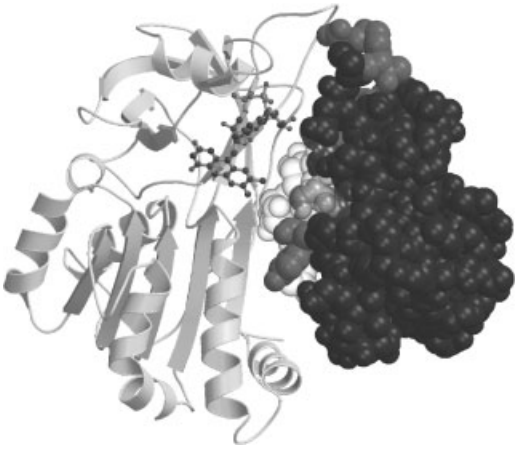

Figure 10. The complex of ferredoxin and ferredoxin-NADP$^+$ oxidoreductase. The complex of maize Fd and FNR (PDB entry 1gaq; Kurisu *et al.*, 2001) is shown, with FNR in ribbons, the FAD cofactor in ball-and-stick, and Fd in spacefilling representation. The residues that are invisible in the NMR spectrum due to paramagnetic relaxation are shown as transparent spheres, with the iron-sulphur cluster of Fd shining through in light grey. The residues affected by binding (according to the NMR results) are in grey and the unaffected residues are in black. The figure was generated with the programmes MOLSCRIPT (Kraulis, 1991) and Raster 3D (Merrit and Bacon, 1997).

FERREDOXIN–FERREDOXIN–NADP$^+$ OXIDOREDUCTASE

Plant-type ferredoxin (Fd) is a small (11 kDa) one-electron carrier protein that contains a single [2Fe–2S] cofactor. It occurs in plants, algae and cyanobacteria and serves as the electron donor to several Fd-dependent enzymes, such as Fd-NADP$^+$ oxidoreductase (FNR). The X-ray structures of several [2Fe–2S]–Fds are available. These include the structure of the protein from the cyanobacterium *Spirulina platensis* Fd (Fukuyama *et al.*, 1980; Fukuyama *et al.*, 1995; PDB entry 4fxc) and that of the Glu92Lys mutant of spinach Fd (Binda *et al.*, 1998; PDB entry 1a70), and reveal a high degree of structural conservation amongst this class of proteins (Akashi *et al.*, 1999). FNR catalyses the conversion of NADP$^+$ into NADPH upon receiving one electron from each of two molecules of Fd. This enzyme contains a flavin adenine dinucleotide (FAD) redox active prosthetic group. The X-ray structure of spinach (Karplus *et al.*, 1991; Bruns and Karplus, 1995; PDB entries 1fnb and 1frn) and maize (Kurisu *et al.*, 2001; PDB entry 1gaw) FNRs are available.

The complexes of maize leaf Fd and FNR have been studied by a combination of X-ray diffraction and NMR spectroscopy. The X-ray structure of the complex formed between the two proteins (Kurisu *et al.*, 2001; PDB entry 1gaq) revealed that the cofactors in Fd and FNR are in close proximity (6 Å) to each other (Fig. 10). Approximately 50% of the 47 residues in the interface between the two proteins are polar. Five Fd residues (Tyr37, Cys39, Ala41, Cys44 and Tyr63) and four FNR residues (Val92, Leu94, Val151 and Val313) at the intermolecular contact region form a hydrophobic region, near the two prosthetic groups (Depascalis *et al.*, 1993; Akashi *et al.*, 1999; Hurley *et al.*, 1999; Matsumura *et al.*, 1999; Kurisu *et al.*, 2001).

NMR chemical-shift perturbation experiments were used to map the sites of Fd that interact with FNR in solution (Kurisu *et al.*, 2001). The largest chemical-shift changes (between 0.2 and 0.4 ppm) were observed for Tyr37 and the regions around Asp60 and Asp65. This is in good agreement with the contact sites found for Fd in the crystal structure of the complex, showing that the binding mode of Fd in the crystal is similar to that found in solution.

It was proposed that electrostatic interactions play an important role in orienting the two proteins and in stabilising the complex (Kurisu *et al.*, 2001). This is in agreement with differential chemical modification studies on spinach Fd (Depascalis *et al.*, 1993), as well as site-directed mutagenesis data obtained for the proteins isolated from maize (Akashi *et al.*, 1999; Matsumura *et al.*, 1999) and *Anabaena* (Hurley *et al.*, 1999). Thus, the contact modes of the two proteins, as observed in the crystal and in solution, suggest an important role of both electrostatic and hydrophobic interactions in complex formation and electron transfer, in accordance with previous laser flash-photolysis studies of the kinetics of reduction of Fd and FNR from *Anabaena* and spinach (Walker *et al.*, 1991).

NADH-PUTIDAREDOXIN REDUCTASE–PUTIDAREDOXIN–CYTOCHROME P450cam

Putidaredoxin (Pdx) is an 11.5 kDa globular protein containing a [2Fe–2S] prosthetic group. Pdx serves as a one-electron shuttle between NADH–putidaredoxin reductase

(PdR; 43.5 kDa) and cytochrome P450cam (CP450cam; 45 kDa; Hintz *et al.*, 1982; Mouro *et al.*, 1999). CP450cam is a haem-containing enzyme that catalyses the 5-exo hydroxylation of camphor in the first step of camphor catabolism in the soil bacterium *Pseudomonas putida*. The two electrons required for camphor hydroxylation by CP450cam come from the oxidation of NADH, which is catalysed by PdR, and are shuttled by Pdx in two distinct electron transfer events. The first of these events is the reduction of substrate (S)-bound CP450cam from the ferric, Fe(III)S, state to the ferrous, Fe(II)S, state. The second reduction event is the reduction of the ferrous oxygenated adduct, O_2–Fe(II)S, which requires the presence of an effector. It has been shown that, in addition to acting as a redox shuttle, Pdx is the *in vivo* physiological effector of CP450cam (Lipscomb *et al.*, 1976).

The first reduction step of CP450cam occurs only after substrate is bound to the cytochrome and can be accomplished by a number of reducing agents with suitable reduction potentials, including bovine adrenodoxin (Adx) and spinach Fd. However, these proteins are unable to serve as effectors for camphor hydroxylation (Lipscomb *et al.*, 1976), suggesting that the second step of CP450cam reduction requires a more specific interaction with Pdx. Cb_5 has been shown to have effector activity for CP450cam but only at concentrations $\sim$20-fold higher than those required for Pdx (Lipscomb *et al.*, 1976).

Two solution structures of Pdx from *Pseudomonas putida* (PDB entries 1put, 1pdx) are available (Pochapsky *et al.*, 1994b, *et al.*, 1999). Several X-ray crystallography structures have been determined for CP450cam, amongst which are those of the free (Poulos *et al.*, 1986) and of the camphor-bound (Poulos *et al.*, 1987) protein (PDB entries 1phc and 2cpp, respectively). Two X-ray structures of PdR have recently been determined (PDB entries 1q1r and 1q1w; Sevrioukova *et al.*, 2004).

The first 2D-NMR investigation of the complex formed between Pdx and CP450cam was carried out by Pochapsky *et al.* (1996). Under the low-salt conditions used in the experiments, the Pdx–CP450cam complex was found to be in the intermediate exchange regime. The amide resonances of the Pdx residues affected by the addition of CP450cam were either shifted or broadened beyond detection. These include several residues that are partially or fully solvent exposed, with a significant number of residues located in the C-terminal region of the protein and several other residues. The authors conclude that many sites on Pdx are affected by the presence of CP450cam and that the initial complexation process is probably non-selective (Pochapsky *et al.*, 1996), in agreement with the promiscuity of CP450cam regarding its initial reduction step. It is postulated that specificity would be enforced by the second electron transfer and/or the effector activity. Chemical modification (Sligar *et al.*, 1974) and site-directed mutagenesis (Davies and Sligar, 1992) studies have shown that Trp106, the C-terminal residue of Pdx, plays a very important role in complex formation with CP450cam. Pochapsky and co-workers postulate that an aromatic–aromatic interaction takes place between Trp106 in Pdx and Tyr78 in CP450cam, the latter being the only aromatic residue on the proximal haem side of CP450cam, which is assumed to be the most likely site of interaction of CP450cam with Pdx (Pochapsky *et al.*, 1996). It was also proposed that electron transfer is facilitated by the closest possible approach between the iron in the [2Fe–2S] cluster closest to the surface of Pdx and the haem iron in CP450cam. Based on these assumptions, molecular dynamics calculations were used to generate a model of the complex between these two proteins. In this model, the main interactions that are responsible for complex formation are of electrostatic nature and, aside from the postulated aromatic–aromatic interactions, no other hydrophobic interactions are observed (Pochapsky *et al.*, 1996). It should be noted, however, that this model was constructed based upon the structures of the oxidized forms of both proteins, thus not the physiologically relevant oxidation states. Evidence is available that clearly shows that there are structural and dynamic differences between oxidized and reduced Pdx (Pochapsky *et al.*, 1994a) and it has been suggested that the somewhat more compact structure of the latter might contribute to its tighter binding to CP450cam than that experienced by the former (Sligar and Gunsalus, 1976; Hintz *et al.*, 1982).

Subsequent 2D-NMR spectroscopy work by Aoki *et al.* (1998b) confirmed the involvement of residues located near the [2Fe–2S] cluster, or near the D-helix and the C-terminal region of Pdx in the interaction with CP450cam. The authors note that some of the amino acid residues affected are specific to Pdx and are not highly conserved in the family of iron–sulphur electron transfer proteins. It is suggested that this low homology may reduce the cross-reactivity to CP450cam by other iron–sulphur proteins (Lipscomb *et al.*, 1976) and that these residues are responsible for the highly specific interactions that occur between Pdx and CP450cam (Aoki *et al.*, 1998b).

Very recently, the investigation of the Pdx–CP450cam interaction was extended by using TROSY-based NMR methods to achieve the ^{1}H, ^{15}N and ^{13}C assignments of CP450cam and by monitoring the perturbations in the [^{1}H,^{15}N]-HSQC spectrum of this protein upon addition of Pdx (Pochapsky *et al.*, 2003). The titration of camphor-bound, oxidized CP450cam with oxidized Pdx did not yield significant changes in the [^{1}H,^{15}N]-HSQC spectrum of the latter, in accordance with previous studies that indicated that this non-physiological complex is relatively weak (Sligar and Gunsalus, 1976; Hintz *et al.*, 1982). However, significant spectral changes were observed when camphor-bound, CO-bound, reduced CP450cam was titrated with reduced Pdx. These effects fall in two different categories: (1) resonances that show both chemical-shift and linewidth changes as Pdx is added, corresponding to perturbations in fast exchange; and (2) resonances that disappear upon the first addition of Pdx, corresponding to perturbations that fall in the intermediate exchange regime. Figure 11 shows the distribution of these perturbations on the CP450cam molecule. As can be seen in this figure, residues in category 1 are distributed throughout several regions of the CP450cam, whereas residues in category 2 are located in the active site or nearby the haem. The results clearly show that, contrary to the initial assumption (Pochapsky *et al.*, 1996), it is not only the proximal face of CP450cam that is perturbed by the interaction with Pdx. On the other hand, the spectral perturbations described are not observed upon addition of Adx to CP450cam but many of them do occur when Cb_5 is added. The fact that Adx is not an effector for CP450cam

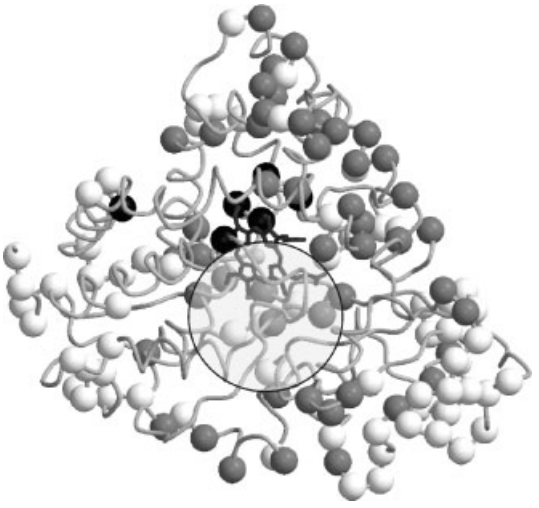

Figure 11. Structure of camphor-bound CP450cam. The residues are represented according to the perturbations caused by Pdx binding. White spheres, residues that are unperturbed by Pdx addition; grey spheres, residues that are shifted upon addition of Pdx; black spheres, residues that are broadened beyond detection upon addition of Pdx. Residues shown as a coil are those for which insufficient data are available. The haem group is shown in sticks. The transparent circle represents the location of Pdx in the molecular dynamics model proposed by Pochapsky and coworkers (Pochapsky *et al.*, 1996; Pochapsky *et al.*, 2003). The figure was generated on the basis of PDB entry 2cpp (Poulos *et al.*, 1987) with the programmes MOLSCRIPT (Kraulis, 1991) and Raster 3D (Merrit and Bacon, 1997).

turnover, whilst Cb_5 can act as such (Lipscomb *et al.*, 1976), suggests that the perturbations observed upon Pdx addition are related to effector activity. The authors propose that the binding of the effector at the proximal face causes perturbations that are not necessarily restricted to the region around the active site. These perturbations would correspond to a selection for a particular subset of conformations of CP450cam that prevent loss of substrate and/or intermediate, resulting in effector activity (Pochapsky *et al.*, 2003). This is in agreement with recent NMR spectroscopy studies (Tosha *et al.*, 2003) that showed that Pdx binding to CP450cam causes D-camphor to approach the haem iron. This Pdx-induced positional change of D-camphor is suggested to lead to its tight binding in the haem pocket, thereby avoiding the loss of substrate in the hydroxylation reaction (Tosha *et al.*, 2003).

The results described in the preceding paragraphs can be summarized as follows: in the first reduction step of CP450cam, Pdx samples a variety of orientations relative to the cytochrome, as shown by the spread binding site on the surface of Pdx (Pochapsky *et al.*, 1996; Aoki *et al.*, 1998b). Specificity is enforced at the second reduction step upon effector activity (Pochapsky *et al.*, 1996, 2003) with residues in the D-helix of Pdx playing a major role in controlling this specificity (Aoki *et al.*, 1998b). The effector activity of Pdx results from the interaction of this protein with the proximal face of CP450cam: this interaction enforces a conformational selection on the cytochrome, enabling turnover (Pochapsky *et al.*, 2003).

The interaction of Pdx with PdR, its other physiological redox partner, was also addressed by Aoki *et al.* (1998b) by means of 2D-NMR. A comparison of the $[^1H,^{15}N]$-HSQC spectra of ^{15}N-labelled, oxidized Pdx in the absence and in the presence of PdR reveals that the resonances from Val28, Glu72, Ile88 and Gln105 are missing from the latter, indicating an involvement of these residues in the binding site with PdR. Previous chemical modification (Geren *et al.*, 1986) and site-directed mutagenesis (Aoki *et al.*, 1998d) studies have implicated Pdx residues Asp58, Glu65, Glu67, Glu77 (Geren *et al.*, 1986) and Glu72 (Geren *et al.*, 1986; Aoki *et al.*, 1998d) in the interaction with PdR, suggesting an important role of the acidic region near the active site of Pdx in the association with PdR. However, a systematic replacement of these residues by site-directed mutagenesis has shown that, with the exception of Glu72, the neutralization of the negative charges did not significantly inhibit the electron-transfer reaction with the PdR (Aoki *et al.*, 1998c). Furthermore, isothermal titration calorimetric studies on the associations of Pdx with PdR suggested an important contribution of hydrophobic interactions to complex formation (Aoki *et al.*, 1998a). In the NMR experiments described above (Aoki *et al.*, 1998b), Glu72 is the only acidic residue found to be significantly affected by PdR, whereas two of the remaining three are hydrophobic residues. For these reasons, the authors conclude that dominant interactions in the Pdx–PdR couple are of hydrophobic rather than electrostatic nature (Aoki *et al.*, 1998b) and suggest that this is reflected in the low cross reactivity observed with the related Adx–adrenodoxin reductase (AdR) system (Geren *et al.*, 1986), where electrostatics are believed to play a major role (Geren *et al.*, 1984).

ADRENODOXIN AND CYTOCHROME *c*

The non-physiological interaction of Adx with Cc has also been the subject of a detailed NMR spectroscopy study. Adx is a 14.4 kDa protein that belongs to the family of vertebrate-type [2Fe–2S] ferredoxins. It occurs in the adrenal mitochondria of vertebrates where it plays a crucial role in steroid hormones biosynthesis by acting as a shuttle between NADPH-dependent adrenodoxin reductase AdR and several cytochromes P450, including cytochrome P450scc (CP450scc), which catalyses the sidechain cleavage of cholesterol (Bernhardt, 1996; Grinberg *et al.*, 2000). The X-ray structures of the wild type (Ziegler *et al.*, 1999) and a truncated (Müller *et al.*, 1998) form of adrenodoxin are available (PDB entries 1cjc and 1ayf, respectively), as well as those of AdR (Ziegler and Schulz, 2000; PDB entry 1e1k) and of the cross-linked complex of AdR and Adx (Müller *et al.*, 2001; PDB entry 1e6e). Adx comprises two domains, termed the core and recognition domains. The former contains the Fe–S cluster and includes residues 5–55 and 91–108, while the latter bears the key residues involved in the recognition of AdR and CP450scc (Müller *et al.*, 1998).

Mitochondrial Cc has been used as the final electron acceptor in a sequential electron transfer route from AdR to the cytochrome, via Adx. Since the reaction between AdR and Adx is the rate-limiting step in this pathway, the electron transfer rate between these two proteins can be

determined by following the reduction of yeast Cc (Lambeth and Kamin, 1979). The observation that electron transfer occurs rapidly between Adx and Cc suggested that a non-physiological complex is formed between these two proteins and prompted a solution NMR spectroscopy investigation of their interaction (Worrall *et al.*, 2003). In these studies, ^{15}N-labelling of both Adx and Cc enabled monitoring of the effects of complex formation on both proteins. The chemical-shift maps obtained upon titration of unlabelled Adx with ^{15}N-labelled Cc and those obtained upon titration of ^{15}N-labelled Adx with unlabelled Cc are shown in Figure 12(A) and (B), respectively. In both cases, a general broadening of the resonances and significant chemical-shift changes were observed, indicating that the interaction is in the fast exchange regime. Most of the affected residues on Cc are located on the front face of the protein, in the region located around the exposed haem edge. However, chemical-shift perturbations were also observed for residues located at the rear of the protein. In the case of the Adx protein, the binding effects are experienced by 41 residues. These residues are located in both domains of Adx, with the largest effects being felt by residues in the recognition domain. A small number of residues in the C-terminal stretch of Adx are also affected by complex formation with Cc, suggesting that this region might be involved in the interaction. Polar, hydrophobic and charged residues on both proteins experience chemical-shift perturbations upon complex formation.

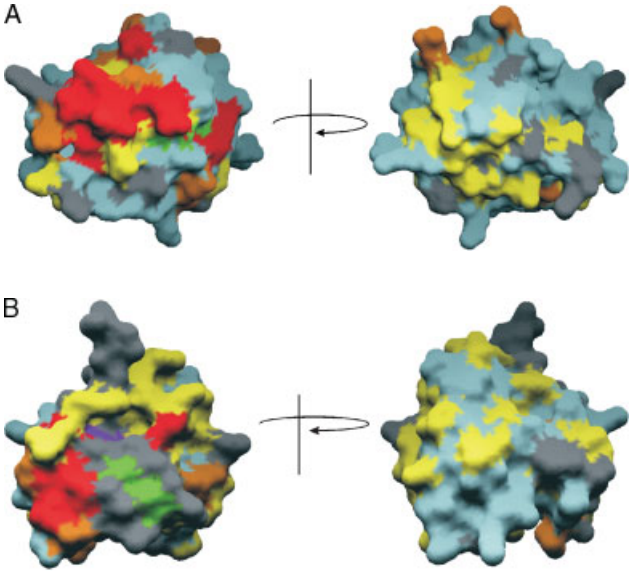

Figure 12. The complex of adrenodoxin and cytochrome *c*. (A) Chemical-shift mapping of Cc in the presence of oxidised Adx and (B) chemical-shift mapping of oxidised Adx in the presence of ferrous Cc. Residues are colour coded according to the chemical-shift perturbation resulting from the presence of the partner protein: red for $\geq$0.03 ppm, orange for $\geq$0.02 ppm, yellow for $\geq$0.01 ppm and blue for $<$0.01 ppm. Unassigned and proline residues are in grey. The haem (A) and two of the active site Cys residues (Cys46 and Cys52, B) are coloured in green. The surfaces on the right have been rotated 180° around the vertical axis, with respect to those on the left. Reprinted in part with permission from Worrall *et al.* (2003). Copyright (2003) American Chemical Society.

The results clearly support the notion that the Adx–Cc complex is a dynamic ensemble of orientations, with both proteins sampling other surface areas, away from the predominant binding sites (state B in Fig. 3).

CONCLUSIONS AND OUTLOOK

The use of 2D-NMR spectroscopy for the characterisation of transient complexes of redox proteins has yielded new insights into the process of complex formation. The striking variation in the size of the chemical-shift perturbations between various complexes suggests that some complexes exist entirely in a non-specific state, consisting of a dynamic ensemble of orientations. These complexes show very small perturbations as a consequence of the averaged and weak molecular interactions. Yet, complex formation is evident in these cases from the increased correlation time (Worrall *et al.*, 2002). Dynamic complexes are still poorly characterized. The rate of the dynamic behaviour within the complex is unknown and could vary from the low ns range to the µs range. It is also unclear how much of the surface of the partner is sampled in the dynamic behaviour.

Complexes that exhibit larger chemical-shift perturbations are assumed to spend at least part of the time in a well-defined orientation within the complex. Stronger molecular interactions and changes in the solvation of the protein surface may be the main reasons for the observed perturbations. Kinetic studies have shown that, in many cases, electrostatic interactions are important for the affinity between the partners. The NMR spectroscopy studies discussed here show that, in particular, uncharged polar as well as hydrophobic residues exhibit the largest chemical-shift perturbations. These results are interpreted as follows (Crowley and Ubbink, 2003; Fig. 13). For the formation of a well-defined complex, hydrophobic interactions are a necessity. To keep the complex transient, extensive desolvation is, however, to be avoided, by limiting the size of the hydrophobic patch and surrounding it with polar residues, which enhance resolvation and, thus, dissociation of the

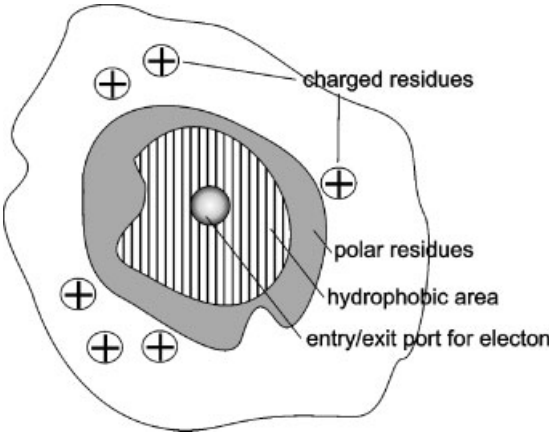

Figure 13. Schematic representation of the interface of a transient redox complex. The entry/exit port for electrons is surrounded by a set of hydrophobic residues, which are lined with polar residues. Charged residues are found on the edge of the binding site.

complex. In most cases, though not all, charged residues surround the binding site or form a separate patch that functions to preorient the partners in approximately the right orientation. In this way the number of collisions that result in an active complex is enhanced, resulting in higher affinity. Desolvation of charged groups is not favourable and salt bridge formation appears not to be a requirement for transient complex formation. In fact, the long-range nature of the electrostatic force may restrict the precision in which the proteins can be oriented. Thus, the hydrophobic interactions are required to bring the entry/exit ports for the electrons of both redox proteins in close contact. Only in this way can rapid electron transfer from one redox centre to the next occur. A general observation of the studies discussed above is that this entry/exit port is located inside the hydrophobic part of the interface, with the exposed haem edge in Cc being perhaps the most well-known example.

Little is still known about 'switch mechanisms' in transient redox complexes. In only a few cases is it clear whether the affinity and the structure of the complex are dependent on the redox state, i.e. whether differences exist between the reactant and product complexes. The work on the complex of Pdx and CP450 demonstrates that subtle switch mechanisms can occur even in weak complexes. Generally, it is difficult to study such effects, because the physiological redox states will rapidly react, while the NMR spectroscopy must study the equilibrium state. Substitution of the redox active metals or other cofactors with redox inactive mimics can be useful, as shown for the complex of Pc and Cf (Ubbink *et al.*,1998), but it is important to test whether the substitution affects the switch mechanism of interest.

Many studies described here apply the chemical-shift perturbation technique. It can be expected that also other NMR methods will be used more extensively for the study of transient complexes. ^{15}N relaxation provides information about dynamics on both ns and high μs timescale (Akke, 2002) and can be used to establish the rotational correlation time. Hydrogen exchange can be applied to determine the degree of protection of amides in the interface of a complex (Jeng *et al.*, 1994; Yi *et al.*, 1994b). Cross-relaxation can help to identify the binding sites in complexes in slow exchange (Takahashi *et al.*, 2000). Finally, paramagnetism can be useful to characterize protein–protein complexes. Paramagnetic shifts can provide information about the orientation of the proteins within the complex (Guiles *et al.*, 1996; Ubbink *et al.*, 1998) and paramagnetic relaxation was recently shown to be a useful tool for mapping binding sites in very weak complexes (Hansen *et al.*, 2003). The use of paramagnetism is particularly appropriate for redox proteins, because it takes advantage of their natural properties. It can be expected that application of all these methods will yield many more interesting details about these transient and highly dynamic protein complexes.

Note

A systematic analysis of interfaces of transient protein complexes based on crystal structures has been published very recently: Crowley P, Carrondo, MA. 2004. *Proteins: Struct. Func. Bioinform.* **55**: 603–612.

Acknowledgements

G.W. Canters, D.S. Bendall, J.A.R. Worrall and P.B. Crowley are acknowledged for fruitful discussions.

REFERENCES

Akashi T, Matsumura T, Ideguchi T, Iwakiri K, Kawakatsu T, Taniguchi I, Hase T. 1999. Comparison of the electrostatic binding sites on the surface of ferredoxin for two ferredoxin-dependent enzymes, ferredoxin–NADP(+) reductase and sulfite reductase. *J. Biol. Chem.* **274**: 29399–29405.

Akke M. 2002. NMR methods for characterizing microsecond to millisecond dynamics in recognition and catalysis. *Curr. Opin. Struct. Biol.* **12**: 642–647.

Aoki M, Ishimori K, Fukada H, Takahashi K, Morishima I. 1998a. Isothermal titration calorimetric studies on the associations of putidaredoxin to NADH-putidaredoxin reductase and P450cam. *Biochim. Biophys. Acta* **1384**: 180–188.

Aoki M, Ishimori K, Morishima I. 1998b. NMR studies of putidaredoxin: associations of putidaredoxin with NADH-putidaredoxin reductase and cytochrome P450cam. *Biochim. Biophys. Acta* **1386**: 168–178.

Aoki M, Ishimori K, Morishima I. 1998c. Roles of negatively charged surface residues of putidaredoxin in interactions with redox partners in p450cam monooxygenase system. *Biochim. Biophys. Acta* **1386**: 157–167.

Aoki M, Ishimori K, Morishima I, Wada Y. 1998d. Roles of valine-98 and glutamic acid-72 of putidaredoxin in the electron-transfer complexes with NADH-putidaredoxin reductase and P450cam. *Inorg. Chim. Acta* **272**: 80–88.

Aubert C, Brugna M, Dolla A, Bruschi M, Giudici-Orticoni MT. 2000. A sequential electron transfer from hydrogenases to cytochromes in sulfate-reducing bacteria. *Biochim. Biophys. Acta* **1476**: 85–92.

Babu CR, Volkman BF, Bullerjahn GS. 1999. NMR solution structure of plastocyanin from the photosynthetic prokaryote. *Prochlorothrix hollandica. Biochemistry* **38**: 4988–4995.

Banci L, Bertini I, Felli IC, Krippahl L, Kubicek K, Moura JJG, Rosato A. 2003. A further investigation of the cytochrome b_5-cytochrome *c* complex. *J. Biol. Inorg. Chem.* **8**: 777–786.

Berghuis AM, Brayer GD. 1992. Oxidation state-dependent conformational changes in cytochrome *c*. *J. Mol. Biol.* **223**: 959–976.

Bergkvist A, Ejdebäck M, Ubbink M, Karlsson G. 2001. Surface interactions in the complex between cytochrome *f* and the E43Q/D44N and E59K/E60Q plastocyanin double mutants as determined by ^1H NMR chemical shift analysis. *Protein Sci.* **10**: 2623–2626.

Bernhardt R. 1996. Cytochrome P450: structure, function, and generation of reactive oxygen species. *Rev. Physiol. Biochem. Pharmac.* **127**: 137–221.

Bertini I, Luchinat C. 1996. NMR of paramagnetic substances. *Coord. Chem. Rev.* **150**: 1–300.

Binda C, Coda A, Aliverti A, Zanetti G, Mattevi A. 1998. Structure of the mutant E92K of [2Fe–2S] ferredoxin I from *Spinacia oleracea* at 1.7 Å resolution. *Acta Crystallogr. D: Biol. Crystallogr.* **54**: 1353–1358.

Blackledge MJ, Medvedeva S, Poncin M, Guerlesquin F, Bruschi M, Marion D. 1995. Structure and dynamics of ferrocytochrome c_{553} from *Desulfovibrio vulgaris* studied by NMR-spectroscopy and restrained molecular-dynamics. *J. Mol. Biol.* **245**: 661–681.

Blanchard L, Payan F, Oian MX, Haser R, Noailly M, Bruschi M, Guerlesquin F. 1993. Intramolecular electron-transfer in ferredoxin-II from *Desulfovibrio desulfuricans* Norway. *Biochim. Biophys. Acta* **1144**: 125–133.

Bruns CM, Karplus PA. 1995. Refined crystal structure of spinach ferredoxin reductase at 1.7 Å resolution—oxidized, reduced and 2′-phospho-5′-AMP-bound states. *J. Mol. Biol.* **247**: 125–145.

Cambillau C, Frey M, Mosse J, Guerlesquin F, Bruschi M. 1988. Model of a complex between the tetrahemic cytochrome c_3 and the ferredoxin I from *Desulfovibrio desulfuricans* (Norway strain). *Proteins* **4**: 63–70.

Crowley PB, Ubbink M. 2003. Close encounters of the transient kind: protein interactions in the photosynthetic redox chain investigated by NMR spectroscopy. *Acc. Chem. Res.* **36**: 723–730.

Crowley PB, Otting G, Schlarb-Ridley BG, Canters GW, Ubbink M. 2001. Hydrophobic interactions in a cyanobacterial plastocyanin–cytochrome *f* complex. *J. Am. Chem. Soc.* **123**: 10444–10453.

Crowley PB, Diaz-Quintana A, Molina-Heredia FP, Nieto P, Sutter M, Haehnel W, De la Rosa MA, Ubbink M. 2002a. The interactions of cyanobacterial cytochrome c_6 and cytochrome *f*, characterized by NMR. *J. Biol. Chem.* **277**: 48685–48689.

Crowley PB, Rabe KS, Worrall JAR, Canters GW, Ubbink M. 2002b. The ternary complex of cytochrome *f* and cytochrome *c*: identification of a second binding site and competition for plastocyanin binding. *ChemBioChem* **3**: 526–533.

Crowley PB, Vintonenko N, Bullerjahn GS, Ubbink M. 2002c. Plastocyanin-cytochrome *f* interactions: the influence of hydrophobic patch mutations studied by NMR spectroscopy. *Biochemistry* **41**: 15698–15705.

Czjzek M, ElAntak L, Zamboni V, Morelli X, Dolla A, Guerlesquin F, Bruschi M. 2002. The crystal structure of the hexadecaheme cytochrome Hmc and a structural model of its complex with cytochrome c(3). *Structure* **10**: 1677–1686.

Davies MD, Sligar SG. 1992. Genetic variants in the putidaredoxin pytochrome P450(Cam) electron-transfer complex—identification of the residue responsible for redox state-dependent conformers. *Biochemistry* **31**: 11383–11389.

Depascalis AR, Jelesarov I, Ackermann F, Koppenol WH, Hirasawa M, Knaff DB, Bosshard HR. 1993. Binding of ferredoxin to ferredoxin–$NADP^+$ oxidoreductase—the role of carboxyl groups, electrostatic surface potential, and molecular dipole-moment. *Protein Sci.* **2**: 1126–1135.

Durley RCE, Mathews FS. 1996. Refinement and structural analysis of bovine cytochrome b_5 at 1.5 angstrom resolution. *Acta Crystallogr D* **52**: 65–76.

Ejdebäck M, Bergkvist A, Karlsson BG, Ubbink M. 2000. Side-chain interactions in the plastocyanin-cytochrome *f* complex. *Biochemistry* **39**: 5022–5027.

ElAntak L, Morelli X, Bornet O, Hatchikian C, Czjzek M, Alain DA, Guerlesquin F. 2003. The cytochrome c_3-[Fe]-hydrogenase electron-transfer complex: structural model by NMR restrained docking. *FEBS Lett.* **548**: 1–4.

Fernandez C, Wider G. 2003. TROSY in NMR studies of the structure and function of large biological macromolecules. *Curr. Opin. Struct. Biol.* **13**: 570–580.

Freeman HC, Guss JM. 2001. Plastocyanin. In *Handbook of Metalloproteins*, Messerschmidt A, Huber R, Poulos TL, Wieghardt K (eds). Wiley: Chichester; 1153–1169.

Fukuyama K, Hase T, Matsumoto S, Tsukihara T, Katsube Y, Tanaka N, Kanudo M, Wada K, Matsubara H. 1980. Structure of *S. platensis* [2Fe–2S] ferredoxin and evolution of chloroplast-type ferredoxins. *Nature* **286**: 522–524.

Fukuyama K, Ueki N, Nakamura H, Tsukihara T, Matsubara H. 1995. Tertiary structure of [2Fe–2S] ferredoxin from *Spirulina platensis* refined at 2.5 Å resolution—structural comparisons of plant-type ferredoxins and an electrostatic potential analysis. *J. Biochem.* **117**: 1017–1023.

Geren LM, O'Brien P, Stonehuerner J, Millett F. 1984. Identification of specific carboxylate groups on adrenodoxin that are involved in the interaction with adrenodoxin reductase. *J. Biol. Chem.* **259**: 2155–2160.

Geren L, Tuls J, O'Brien P, Millett F, Peterson JA. 1986. The involvement of carboxylate groups of putidaredoxin in the reaction with putidaredoxin reductase. *J. Biol. Chem.* **261**: 15491–15495.

Goodfellow BJ, Macedo AL, Rodrigues P, Moura I, Wray V, Moura JJG. 1999. The solution structure of a [3Fe–4S] ferredoxin: oxidized ferredoxin II from *Desulfovibrio gigas*. *J. Biol. Inorg. Chem.* **4**: 421–430.

Grinberg AV, Hannemann F, Schiffler B, Müller J, Heinemann U, Bernhardt R. 2000. Adrenodoxin: structure, stability, and electron transfer properties. *Proteins* **40**: 590–612.

Guiles RD, Sarma S, DiGate RJ, Banville D, Basus VJ, Kuntz ID, Waskell L. 1996. Pseudocontact shifts used in the restraint of the solution structures of electron transfer complexes. *Nat. Struct. Biol.* **3**: 333–339.

Hagler L, Coppes RI, Herman RH. 1979. Metmyoglobin reductase. *J. Biol. Chem.* **254**: 6505–6514.

Hansen DF, Hass MAS, Christensen HM, Ulstrup J, Led JJ. 2003. Detection of short-lived transient protein–protein interactions by intermolecular nuclear paramagnetic relaxation: plastocyanin from *Anabaena variabilis*. *J. Am. Chem. Soc.* **125**: 6858–6859.

Hart SE, Schlarb-Ridley BG, Delon C, Bendall DS, Howe CJ. 2003. Role of charges on cytochrome *f* from the cyanobacterium *Phormidium laminosum* in its interaction with plastocyanin. *Biochemistry* **42**: 4829–4836.

Hervás M, Navarro JA, De la Rosa MA. 2003. Electron transfer between membrane complexes and soluble proteins in photosynthesis. *Acc. Chem. Res.* **36**: 798–805.

Hintz MJ, Mock DM, Peterson LL, Tuttle K, Peterson JA. 1982. Equilibrium and kinetic studies of the interaction of cytochrome P-450cam and putidaredoxin. *J. Biol. Chem.* **257**: 14324–14332.

Hom K, Ma QF, Wolfe G, Zhang H, Storch EM, Daggett V, Basus VJ, Waskell L. 2000. NMR studies of the association of cytochrome b_5 with cytochrome *c*. *Biochemistry* **39**: 14025–14039.

Hope AB. 2000. Electron transfers amongst cytochrome *f*, plastocyanin and photosystem I: kinetics and mechanisms. *Biochim. Biophys. Acta Bioenerg.* **1456**: 5–26.

Hurley JK, Hazzard JT, Martínez-Júlvez M, Medina M, Gómez-Moreno C, Tollin G. 1999. Electrostatic forces involved in orienting *Anabaena* ferredoxin during binding to *Anabaena* ferredoxin: $NADP^+$ reductase: site-specific mutagenesis, transient kinetic measurements, and electrostatic surface potentials. *Protein Sci.* **8**: 1614–1622.

Illerhaus J, Altschmied L, Reichert J, Zak E, Herrmann RG, Haehnel W. 2000. Dynamic interaction of plastocyanin with the cytochrome *bf* complex. *J. Biol. Chem.* **275**: 17590–17595.

Jeng MF, Englander SW, Pardue K, Rogalskyj JS, McLendon G. 1994. Structural dynamics in an electron-transfer complex. *Nat. Struct. Biol.* **1**: 234–238.

Karplus PA, Daniels MJ, Herriott JR. 1991. Atomic structure of ferredoxin-$NADP^+$ reductase—prototype for a structurally novel flavoenzyme family. *Science* **251**: 60–66.

Kissinger CR, Sieker LC, Adman ET, Jensen LH. 1991. Refined crystal structure of ferredoxin-II from *Desulfovibrio gigas* at 1.7 Å. *J. Mol. Biol.* **219**: 693–715.

Kraulis PJ. 1991. MOLSCRIPT: a program to produce both detailed and schematic plots of protein structures. *J. Appl. Crystallogr.* **24**: 946–950.

Krippahl L, Moura JJ, Palma PN. 2003. Modeling protein complexes with BiGGER. *Proteins* **52**: 19–23.

Kurisu G, Kusunoki M, Katoh E, Yamazaki T, Teshima K, Onda Y, Kimata-Ariga Y, Hase T. 2001. Structure of the electron transfer complex between ferredoxin and ferredoxin-$NADP(+)$ reductase. *Nat. Struct. Biol.* **8**: 117–121.

Kurisu G, Zhang HM, Smith JL, Cramer WA. 2003. Structure of the cytochrome b_6f complex of oxygenic photosynthesis: tuning the cavity. *Science* **302**: 1009–1014.

Lambeth JD, Kamin H. 1979. Adrenodoxin reductase-adrenodoxin complex: flavin to iron-sulfur electron transfer as the rate-limiting step in the NADPH-cytochrome *c* reductase reaction. *J. Biol. Chem.* **254**: 2766–2774.

Leesch VW, Bujons J, Mauk AG, Hoffman BM. 2000. Cytochrome *c* peroxidase cytochrome *c* complex: locating the second binding domain on cytochrome *c* peroxidase with site-directed mutagenesis. *Biochemistry* **39**: 10132–10139.

Liang ZX, Nocek JM, Huang K, Hayes RT, Kurnikov IV, Beratan DN, Hoffman BM. 2002. Dynamic docking and electron transfer between Zn-myoglobin and cytochrome b_5. *J. Am. Chem. Soc.* **124**: 6849–6859.

Lipscomb JD, Sligar SG, Namtvedt MJ, Gunsalus IC. 1976. Autooxidation and hydroxylation reactions of oxygenated cytochrome P-450cam. *J. Biol. Chem.* **251**: 1116–1124.

Livingston DJ, McLachlan SJ, La Mar GN, Brown WD. 1985. Myoglobin: cytochrome b_5 interactions and the kinetic mechanism of metmyoglobin reductase. *J. Biol. Chem.* **260**: 15699–15707.

Marion D, Blackledge MJ, Brutscher B, Guerlesquin F, Bersch B, Meyer TE. 1995. NMR structure determination of cytochrome-c_{553} of *Desulfovibrio vulgaris* Hildenborough and cytochrome-c_{551} of *Ectothiorhodospira halophila. J. Cell. Biochem.* Suppl. 21B: 29.

Matsumura T, Kimata-Ariga Y, Sakakibara H, Sugiyama T, Murata H, Takao T, Shimonishi Y, Hase T. 1999. Complementary DNA cloning and characterization of ferredoxin localized in bundle-sheath cells of maize leaves. *Plant Physiol.* **119**: 481–488.

Merrit EA, Bacon DJ. 1997. Raster3D photorealistic molecular graphics. *Meth. Enzymol.* **277**: 505–524.

Moench SJ, Chroni S, Lou BS, Erman JE, Satterlee JD. 1992. Proton NMR comparison of noncovalent and covalently cross-linked complexes of cytochrome *c* peroxidase with horse, tuna, and yeast ferricytochromes *c. Biochemistry* **31**: 3661–3670.

Morelli X, Guerlesquin F. 1999. Mapping the cytochrome c_{553} interacting site using ^{1}H and ^{15}N NMR. *FEBS Lett.* **460**: 77–80.

Morelli X, Czjzek M, Hatchikian CE, Bornet O, Fontecilla-Camps JC, Palma NP, Moura JJG, Guerlesquin F. 2000a. Structural model of the Fe-hydrogenase/cytochrome c_{553} complex combining transverse relaxation-optimized spectroscopy experiments and soft docking calculations. *J. Biol. Chem.* **275**: 23204–23210.

Morelli X, Dolla A, Czjzek M, Palma PN, Blasco F, Krippahl L, Moura JJG, Guerlesquin F. 2000b. Heteronuclear NMR and soft docking: an experimental approach for a structural model of the cytochrome c_{553}–ferredoxin complex. *Biochemistry* **39**: 2530–2537.

Morelli XJ, Palma PN, Guerlesquin F, Rigby AC. 2001. A novel approach for assessing macromolecular complexes combining soft-docking calculations with NMR data. *Protein Sci.* **10**: 2131–2137.

Mouro C, Bondon A, Jung C, Hoa GHB, De Certaines JD, Spencer RGS, Simonneaux G. 1999. Proton nuclear magnetic resonance study of the binary complex of cytochrome P450cam and putidaredoxin: interaction and electron transfer rate analysis. *FEBS Lett.* **455**: 302–306.

Müller A, Müller JJ, Muller YA, Uhlmann H, Bernhardt R, Heinemann U. 1998. New aspects of electron transfer revealed by the crystal structure of a truncated bovine adrenodoxin, Adx(4–108). *Structure* **6**: 269–280.

Müller JJ, Lapko A, Bourenkov G, Ruckpaul K, Heinemann U. 2001. Adrenodoxin reductase–adrenodoxin complex structure suggests electron transfer path in steroid biosynthesis. *J. Biol. Chem.* **276**: 2786–2789.

Nicolet Y, Piras C, Legrand P, Hatchikian CE, Fontecilla-Camps JC. 1999. *Desulfovibrio desulfuricans* iron hydrogenase: the structure shows unusual coordination to an active site Fe binuclear center. *Struct. Fold. Des.* **7**: 13–23.

Nocek JM, Zhou JS, DeForest S, Priyadarshy S, Beratan DN, Onuchic JN, Hoffman BM. 1996. Theory and practice of electron transfer within protein–protein complexes: application to the multidomain binding of cytochrome *c* by cytochrome *c* peroxidase. *Chem. Rev.* **96**: 2459–2489.

Northrup SH, Thomasson KA, Miller CM, Barker PD, Eltis LD, Guillemette JG, Inglis SC, Mauk AG. 1993. Effects of charged amino-acid mutations on the bimolecular kinetics of reduction of yeast iso-1-ferricytochrome *c* by bovine ferrocytochrome b_5. *Biochemistry* **32**: 6613–6623.

Palma PN, Krippahl L, Wampler JE, Moura JJG. 2000. BiGGER: a new (soft) docking algorithm for predicting protein interactions. *Proteins* **39**: 372–384.

Pelletier H, Kraut J. 1992. Crystal structure of a complex between electron transfer partners, cytochrome *c* peroxidase and cytochrome *c. Science* **258**: 1748–1755.

Pervushin K, Riek R, Wider G, Wuthrich K. 1997. Attenuated T_2 relaxation by mutual cancellation of dipole-dipole coupling and chemical shift anisotropy indicates an avenue to NMR structures of very large biological macromolecules in solution. *Proc. Natl Acad. Sci. USA* **94**: 12366–12371.

Pochapsky TC, Ratnaswamy G, Patera A. 1994a. Redox-dependent ^{1}H-NMR spectral features and tertiary structural constraints on the C-terminal region ofputidaredoxin. *Biochemistry* **33**: 6433–6441.

Pochapsky TC, Ye XM, Ratnaswamy G, Lyons TA. 1994b. An NMR-derived model for the solution structure of oxidized putidaredoxin, a 2-Fe, 2-S ferredoxin from *Pseudomonas. Biochemistry* **33**: 6424–6432.

Pochapsky TC, Lyons TA, Kazanis S, Arakaki T, Ratnaswamy G. 1996. A structure-based model for cytochrome P450(cam)–putidaredoxin interactions. *Biochimie* **78**: 723–733.

Pochapsky TC, Jain NU, Kuti M, Lyons TA, Heymont J. 1999. A refined model for the solution structure of oxidized putidaredoxin. *Biochemistry* **38**: 4681–4690.

Pochapsky SS, Pochapsky TC, Wei JW. 2003. A model for effector activity in a highly specific biological electron transfer complex: the cytochrome P450(cam)- putidaredoxin couple. *Biochemistry* **42**: 5649–5656.

Poulos TL, Finzel BC, Howard AJ. 1986. Crystal structure of substrate-free *Pseudomonas putida* cytochrome P-450. *Biochemistry* **25**: 5314–5322.

Poulos TL, Finzel BC, Howard AJ. 1987. High-resolution crystal structure of cytochrome P450cam. *J. Mol. Biol.* **195**: 687–700.

Reuter W, Wiegand G. 2001. Cytochrome c_6. In *Handbook of Metalloproteins,* Messerschmidt A, Huber R, Poulos TL, Wieghardt K (eds). Wiley: Chichester; 87–99.

Salemme FR. 1976. An hypothetical structure for an intermolecular electron transfer complex of cytochromes *c* and b_5. *J. Mol. Biol.* **102**: 563–568.

Schlarb-Ridley BG, Bendall DS, Howe CJ. 2002. Role of electrostatics in the interaction between cytochrome *f* and plastocyanin of the cyanobacterium *Phormidium laminosum. Biochemistry* **41**: 3279–3285.

Sebban C, Blanchard L, Bruschi M, Guerlesquin F. 1995. Purification and characterization of the formate dehydrogenase from *Desulfovibrio vulgaris* Hildenborough. *FEMS Microbiol. Lett.* **133**: 143–149.

Sebban-Kreuzer C, Blackledge M, Dolla A, Marion D, Guerlesquin F. 1998a. Tyrosine 64 of cytochrome c_{553} is required for electron exchange with formate dehydrogenase in *Desulfovibrio vulgaris* Hildenborough. *Biochemistry* **37**: 8331–8340.

Sebban-Kreuzer C, Dolla A, Guerlesquin F. 1998b. The formate dehydrogenase-cytochrome c_{553} complex from *Desulfovibrio vulgaris* hildenborough. *Eur. J. Biochem.* **253**: 645–652.

Sevrioukova IF, Li H, Poulos TL. 2004. Crystal structure of putidaredoxin reductase from *Pseudomonas putida*, the final structural component of the cytochrome P450cam monooxygenase. *J. Mol. Biol.* **336**, 889–902.

Shao WP, Im SC, Zuiderweg ERP, Waskell L. 2003. Mapping the binding interface of the cytochrome b_5-cytochrome *c* complex by nuclear magnetic resonance. *Biochemistry* **42**: 14774–14784.

Sligar SG, Gunsalus IC. 1976. A thermodynamic model of regulation: modulation of redox equilibria in camphor monooxygenase. *Proc. Natl Acad. Sci. USA* **73**: 1078–1082.

Sligar SG, Debrunner PG, Lipscomb JD, Namtvedt MJ, Gunsalus IC. 1974. A role of the putidaredoxin COOH-terminus in P-450cam (cytochrome *m*) hydroxylations. *Proc. Natl Acad. Sci. USA* **71**: 3906–3910.

Soriano GM, Ponamarev MV, Tae G-S, Cramer WA. 1996. Effect of the interdomain basic region of cytochrome *f* on its redox reactions *in vivo. Biochemistry* **35**: 14590–14598.

Soriano GM, Smith JL, Cramer WA. 2001. Cytochrome *f*. In *Handbook of Metalloproteins*, Messerschmidt A, Huber R, Poulos TL, Wieghardt K (eds). Wiley: Chichester; 172–181.

Stewart DE, Legall J, Moura I, Moura JJ, Peck HD, Jr, Xavier AV, Weiner PK, Wampler JE. 1989. Electron transport in sulfate-reducing bacteria: molecular modeling and NMR studies of the rubredoxin–tetraheme cytochrome c_3 complex. *Eur. J. Biochem.* **185**: 695–700.

Takahashi H, Nakanishi T, Kami K, Arata Y, Shimada I. 2000. A novel NMR method for determining the interfaces of large protein–protein complexes. *Nat. Struct. Biol.* **7**: 220–223.

Tosha T, Yoshioka S, Takahashi S, Ishimori K, Shimada H, Morishima I. 2003. NMR study on the structural changes of cytochrome P450cam upon the complex formation with putidaredoxin—functional significance of the putidaredoxin-induced structural changes. *J. Biol. Chem.* **278**: 39809–39821.

Ubbink M, Ejdebäck M, Karlsson BG, Bendall DS. 1998. The structure of the complex of plastocyanin and cytochrome *f*, determined by paramagnetic NMR and restrained rigid-body molecular dynamics. *Structure* **6**: 323–335.

Verhagen MFJM, Wolbert RBG, Hagen WR. 1994. Cytochrome c_{553}, from *Desulfovibrio vulgaris* (Hildenborough)—electrochemical properties and electron-transfer with hydrogenase. *Eur. J. Biochem.* **221**: 821–829.

Walker MC, Pueyo JJ, Navarro JA, Gomezmoreno C, Tollin G. 1991. Laser flash-photolysis studies of the kinetics of reduction of ferredoxins and ferredoxin $NADP^+$ reductases from *Anabaena* Pcc-7119 and spinach—electrostatic effects on intracomplex electron-transfer. *Arch. Biochem. Biophys.* **287**: 351–358.

Wienk H, Maneg O, Lucke C, Pristovsek P, Lohr F, Ludwig B, Ruterjans H. 2003. Interaction of cytochrome *c* with cytochrome *c* oxidase: an NMR study on two soluble fragments derived from *Paracoccus denitrificans*. *Biochemistry* **42**: 6005–6012.

Worrall JAR, Kolczak U, Canters GW, Ubbink M. 2001. Interaction of yeast iso-1-cytochrome *c* with cytochrome *c* peroxidase investigated by [N-15,H-1] heteronuclear NMR spectroscopy. *Biochemistry* **40**: 7069–7076.

Worrall JAR, Liu YJ, Crowley PB, Nocek JM, Hoffman BM, Ubbink M. 2002. Myoglobin and cytochrome b_5: a nuclear magnetic resonance study of a highly dynamic protein complex. *Biochemistry* **41**: 11721–11730.

Worrall JAR, Reinle W, Bernhardt R, Ubbink M. 2003. Transient protein interactions studied by NMR spectroscopy: the case of cytochrome *c* and adrenodoxin. *Biochemistry* **42**: 7068–7076.

Yi Q, Erman JE, Satterlee JD. 1994a. H^1-NMR evaluation of yeast isozyme-1 ferricytochrome *c* equilibrium exchange dynamics in noncovalent complexes with 2 forms of yeast cytochrome *c* peroxidase. *J. Am. Chem. Soc.* **116**: 1981–1987.

Yi Q, Erman JE, Satterlee JD. 1994b. Studies of protein–protein association between yeast cytochrome *c* peroxidase and yeast iso-1-ferricytochrome *c* by hydrogen-deuterium exchange labeling and proton NMR spectroscopy. *Biochemistry* **33**: 12032–12041.

Zhou JS, Hoffman BM. 1994. Stern-volmer in reverse: 2:1 stoichiometry of the cytochrome *c*-cytochrome *c* peroxidase electron-transfer complex. *Science* **265**: 1693–1696.

Zhou JS, Nocek JM, Devan ML, Hoffman BM. 1995. Inhibitor-enhanced electron-transfer—copper cytochrome *c* as a redox-inert probe of ternary complexes. *Science* **269**: 204–207.

Ziegler GA, Schulz GE. 2000. Crystal structures of adrenodoxin reductase in complex with $NADP+$ and NADPH suggesting a mechanism for the electron transfer of an enzyme family. *Biochemistry* **39**: 10986–10995.

Ziegler GA, Vonrhein C, Hanukoglu I, Schulz GE. 1999. The structure of adrenodoxin reductase of mitochondrial P450 systems: electron transfer for steroid biosynthesis. *J. Mol. Biol.* **289**: 981–990.

